

Tunnelling through a dynamical barrier in dissipative quantum systems

D Boosé†, J Richert‡ and U Smilansky‡

† Division de Physique Théorique, Centre de Recherches Nucléaires, CNRS/Université Louis Pasteur, BP 20, 67037 Strasbourg Cedex, France

‡ Department of Nuclear Physics, Weizmann Institute of Science, 76 100 Rehovot, Israel

Received 6 February 1992, in final form 14 July 1992

Abstract. Quantum tunnelling induces transitions not only through potential barriers, but also through energy barriers of dynamical origin. The coupling to a noisy environment introduces dissipation which affects tunnelling. This effect is studied by an analytic non-perturbative solution of a problem involving tunnelling through a dynamical barrier in the presence of a noisy environment. The accessibility to the classically forbidden energy region above the dynamical barrier is reduced (enhanced) by the friction (diffusion) effect. The occupation of each level above the dynamical barrier is characterized by the succession in time of two different regimes. The transition between both regimes is ruled by an energy criterion which is discussed.

1. Introduction

The behaviour of quantum systems which are coupled to a dissipative environment is an important subject of research in several fields of physics. Indeed, various physical realizations of such systems can be given. In solid state physics the ever present phonon field is pictured as a dissipative background when considering the macroscopic yet quantal SQUIDS [1]. In atomic physics, molecules and atoms passing through microwave cavities are subject to the superposition of both a coherent signal and a noisy interaction due to black-body radiation [2, 3]. In nuclear physics, collective motion in nuclei is damped by the transfer of energy and angular momentum to the single particle degrees of freedom which act as an effective environment [4]. A recent paper by Hänggi *et al* [5] gives an updated review of the subject and a comprehensive list of references.

The common feature of all these systems lies in the fact that the noisy interaction tends to suppress the effects due to phase coherence, namely interference and tunnelling effects. In the present work we shall be concerned with the latter aspect, namely the influence of a dissipative environment on quantum tunnelling. Caldeira and Leggett [6] were among the first to draw attention to the effects of the environment on tunnelling through a potential barrier. Similar effects were also discussed in nuclear physics in the context of fusion below the Coulomb barrier [7].

It is however possible to think of situations in which ‘tunnelling’ processes occur without the involvement of any actual potential barrier. As a matter of fact, consider the example of a two-level system with a parametric Hamiltonian which varies slowly in time. Even though there is no potential barrier to tunnel through, the occurring

Landau–Zener transition is a tunnelling phenomenon in the sense that it genuinely depends on the wave nature of quantum mechanics. The barrier which is crossed is a dynamical one, whose origin is due to the adiabatic variation of the parameters. The formal analogy between the Landau–Zener effect and ordinary tunnelling is made clear in the elegant treatment of Landau and Lifshitz [8]. It has been shown [9] that the Landau–Zener transition probability is affected in a non-trivial way when the two-level system is coupled to an environment.

This example suggests that one can formally generalize the usual concept of tunnelling to situations where it is a dynamical constraint, rather than a potential hump, which effectively acts as the barrier dividing phase space into distinct regions. While being classically forbidden because of dynamical reasons, transitions between these separate regions are possible because of the wave nature of quantum mechanics. The associated quantum mechanical transition probabilities are exponentially small, just as in the case of ordinary tunnelling [10].

Rainbow scattering is another simple example illustrating the idea. The attractive potential which induces the scattering deflects the classical trajectories (or light rays) in such a way that none of them are scattered into a certain zone which is the classically forbidden region, bounded by a caustic. When one considers the analogous wave scattering problem one finds that the intensity of scattered waves decreases in an exponential way from the illuminated (classically allowed) to the shaded (classically forbidden) region. This transition through the caustic is formally equivalent to the tunnelling through a potential barrier and this analogy may even be pushed further by remembering that both processes can be accounted for in the semi-classical framework by allowing for complex-valued classical trajectories [10, 11]. A third illustrative example comes in the study of the excitation of rotational bands in molecules and nuclei by an external driving torque M which is applied during a finite time interval Δt . Classically the external torque can transfer only a finite amount of angular momentum to the target, which is of the order of (but usually less than) the classical threshold $M\Delta t$. However, because of the quantum nature of the process, one observes transitions to angular momenta higher than the classical threshold. The intensity drops exponentially as the angular momentum increases beyond the classical threshold [12], in much the same way as the rainbow intensity is reduced upon entering the classically forbidden region. Here again one observes a generalized “tunnelling” effect in which it is a dynamical barrier, the classical threshold in angular momentum, rather than a simple potential barrier which is crossed in phase-space.

To summarize the examples just given, we can say that the well-known phenomenon of tunnelling through a potential barrier is only one particular instance of a large variety of situations where classical dynamics precludes certain transitions which nevertheless do occur because of the existence of generalized ‘tunnelling’ processes on the quantum (wave) level. It is interesting to ask how a noisy environment affects these generalized ‘tunnelling’ phenomena when they occur in dissipative systems. The present paper intends to answer this question by studying the effects of such an environment on the probability distribution of classically forbidden transitions. This is done in the framework of a simple model which nevertheless can be thought of as a paradigm for the examples cited earlier.

The model considered here consists of a one-dimensional harmonic oscillator (HO) which is driven by an external time-dependent force $f(t)$. If this force is acting during a given interval of time, the HO can gain only a finite amount of energy. This leads to the existence of two energy thresholds which can be considered as dynamical barriers

bounding an interval of classically allowed energies. However, in agreement with what has been pointed out above, a generalized 'tunnelling' process allows the quantum HO to cross these dynamical barriers and reach the classically forbidden energy ranges [13]. A dissipative system is created by coupling a noisy environment to the driven HO. We present here a non-perturbative analytic expression for the energy distribution associated with the quantum dissipative HO. This expression enables us to study the finite-time effects of dissipation on the population of a classically forbidden energy region, which is the purpose of the paper.

We have to stress that it is possible to obtain an analytic expression of the quantum energy distribution only in the case where the Hamiltonian associated with the dissipative system is quadratic, which is the case considered here. This point raises an issue which has to be settled. Indeed, it is known that the classical and quantum dynamics coincide in phase-space for quadratic Hamiltonians. How can we then expect to see any generalized 'tunnelling' effect in a model whose quantum and classical versions are equivalent? The answer to this apparent paradox is the following. It is true that, in the Cartesian representation of phase-space, the Wigner transform of the quantum evolution operator is identical to the classical Liouville propagator when dealing with quadratic Hamiltonians. However, it must be remembered that for experiments involving microscopic systems it is natural in quantum (classical) mechanics to label the initial and final states of these systems by quantum numbers (classical actions). It is the very projection onto these states that brings in the difference between classical and quantum mechanics, because the square of a projected wavefunction is clearly different from a projected classical phase-space probability distribution. In other words, a Hamiltonian which is quadratic in the Cartesian representation of phase-space is no more so in the action-angle representation of phase-space, which is the natural representation for the present application.

The paper is organized as follows. Section 2 summarizes the well-known results for the case of an isolated driven classical and quantum mechanical HO. The existence of a classically forbidden energy region which may be reached by a generalized 'tunnelling' process is emphasized. In section 3, the system is coupled to a noisy environment. The analytic expression of the quantum energy distribution of the dissipative driven HO is given (the technical details are deferred to the appendixes). In section 4, the finite-time effects of the environment on the tunnelling tail of this distribution are discussed. This is done by comparing the quantum versions of the model with and without environment on the one hand, and the quantum and classical versions of the model with environment on the other hand. A conclusion summarizes the main results of the paper.

2. Energy distributions of the driven HO

We recall here the explicit expressions of the classical and quantum mechanical energy distributions of an HO coupled to a time-dependent external driving force.

2.1. Classical mechanics

The equation of motion for the one-dimensional driven HO is

$$\mu \ddot{q}_{cl}(t) + \mu \omega_0^2 q_{cl}(t) = f(t) \quad (2.1)$$

where μ represents the mass, ω_0 the angular frequency and $f(t)$ the external driving force. In the following, we are interested in finite-time effects of the dissipative environment on the driven HO. Therefore we assume that $f(t)$ acts only in the interval of time between $t=0$ and $t = \Delta t$ and vanishes outside it.

In order to make a consistent comparison between the classical and quantum versions of the model, the HO is prepared at $t=0$ in the same energy state $E_0 = \hbar\omega_0/2$ in both cases. Therefore, in the action-angle representation (I, ϕ) , the initial classical phase-space distribution ρ reads

$$\rho(I, \phi) = \delta(I - I_0)/2\pi. \quad (2.2)$$

with

$$I_0 = \hbar/2.$$

After the excitation of duration Δt , the energy distribution has broadened such that to each initial angle ϕ_0 there corresponds an energy

$$\begin{aligned} E_f(I_0, \phi_0) &= \omega_0 I_f(I_0, \phi_0) \\ &= \omega_0 [I_0 + |F(\Delta t)|^2 + 2\sqrt{I_0}(\cos \phi_0 \operatorname{Re}\{F(\Delta t)\} - \sin \phi_0 \operatorname{Im}\{F(\Delta t)\})] \end{aligned} \quad (2.3)$$

where

$$F(\Delta t) = \frac{1}{\sqrt{2\mu\omega_0}} \int_0^{\Delta t} dt f(t) \exp(i\omega_0 t). \quad (2.3a)$$

The probability distribution in energy is given by

$$\begin{aligned} P^{\text{CL}}(E_f, \Delta t) &= \frac{1}{2\pi} \int_0^{2\pi} \delta(E_f - E_f(I_0, \phi_0)) d\phi_0 \\ &= \frac{1}{\pi} \frac{1}{(4\omega_0 E_0 |F(\Delta t)|^2 - (E_f - E_0 - \omega_0 |F(\Delta t)|^2)^2)^{1/2}}. \end{aligned} \quad (2.4)$$

It is seen that the energies E_f which may be reached by the driven HO are located in the interval

$$E_{\min} = \omega_0 \left(\sqrt{I_0} - \sqrt{|F(\Delta t)|^2} \right)^2 < E_f < \omega_0 \left(\sqrt{I_0} + \sqrt{|F(\Delta t)|^2} \right)^2 = E_{\max}. \quad (2.5)$$

This is the classical accessible region which has already been alluded to in the introduction. The two extrema of the interval are acting as dynamical barriers in phase-space, preventing the system from reaching either lower or higher energies and therefore bounding two classically forbidden regions. The singular behaviour of $P^{\text{CL}}(E_f, \Delta t)$ at these extrema (which is typical of the behaviour shown by classical distribution functions near caustics) does not affect its normalizability. A typical distribution $\{P^{\text{CL}}(E_f, \Delta t)\}$ with its two dynamical barriers is displayed in figure 1.

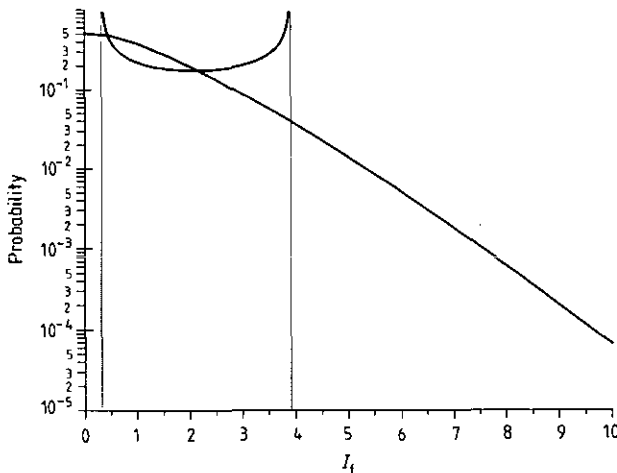


Figure 1. Classical energy distributions $\{P^{CL}(E_f, \Delta t)\}$ and $\{P^{CL,d}(E_f, \Delta t)\}$ as a function of the action $I_f = E_f/\omega_0$. The two vertical lines correspond to the two dynamical barriers of energy E_{min} and E_{max} respectively (cf (2.5)). The distribution $\{P^{CL}(E_f, \Delta t)\}$ is the one within the two barriers. The parameters used here are (in appropriate units) $\mu = 0.5, \hbar = 1.0, \omega_0 = 1.5, \gamma = 1.1, b_0 = 2.2$ and $\Delta t = 3.0$. The external driving force is chosen to be constant with a strength $f_0 = 1.5$.

2.2. Quantum mechanics

Consider an HO which is initially prepared in the state m ($m = 0$ represents the ground state in the following). Its probability to occupy the state n after having been driven during a time Δt is

$$P_{mn}^{QM}(\Delta t) = \left| \int_{-\infty}^{+\infty} dq \int_{-\infty}^{+\infty} dq' \varphi_n^*(q') G(q', \Delta t | q, 0) \varphi_m(q) \right|^2 \tag{2.6}$$

where $G(q', \Delta t | q, 0)$ is the Green function which propagates the system from position q at time 0 to position q' at time Δt and φ_m (φ_n) is the eigenfunction of the HO corresponding to state m (n).

The explicit expression of the occupation probabilities $P_{0n}^{QM}(\Delta t)$ we are interested in here is [14]

$$P_{0n}^{QM}(\Delta t) = \frac{1}{n!} W^{2n}(\Delta t) \exp(-W^2(\Delta t)) \tag{2.7}$$

with

$$W^2(\Delta t) = |F(\Delta t)|^2 / \hbar. \tag{2.7a}$$

Contrary to its classical counterpart (2.4), the Poissonian expression (2.7) presents no singularities and extends over the whole range of energies from the ground state up to infinity. This difference in behaviour is due to the fact that phase coherence is taken into account in (2.6) but not in (2.4). Therefore, as already mentioned in the introduction, a generalized ‘tunnelling’ process across the dynamical barrier of energy E_{max} allows the quantum driven HO to reach the classically forbidden energy

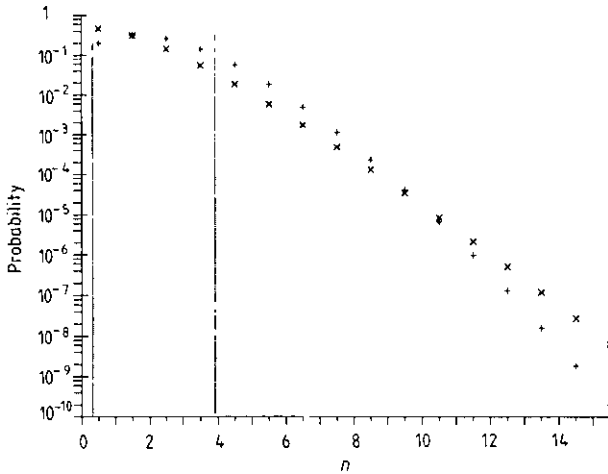


Figure 2. Quantum energy distributions $\{P_{0n}^{QM}(\Delta t)\}$ (+) and $\{P_{0n}^{QM,d}(\Delta t)\}$ (x) as a function of the HO quantum number n (the values of the occupation probabilities are marked at $n + 1/2$). The two vertical lines correspond to the two dynamical barriers. The parameters are the same as those used in figure 1.

region above E_{\max} [13]. So the energy distribution $\{P_{0n}^{QM}(\Delta t)\}$ is characterized by a tunnelling tail extending over the whole classically forbidden energy region. Figure 2 shows an example of such a distribution.

The difference between the classical and quantum versions of the model also appears at the level of the moments associated with the energy distributions. While the classical and quantum mechanical energy averages

$$\langle E(\Delta t) \rangle = E_0 (1 + 2W^2(\Delta t)) \quad (2.8a)$$

and energy variances

$$\langle E^2(\Delta t) \rangle - \langle E(\Delta t) \rangle^2 = 4E_0^2 W^2(\Delta t) \quad (2.8b)$$

are the same, all higher moments are different.

3. Energy distributions of the dissipative driven HO

We consider now the case of interest in this paper, i.e. the dissipative system formed by the driven HO coupled to a noisy environment. As in the theory of Brownian motion this environment is characterized by a friction force and a correlation function $b(t-t') = \langle L(t)L(t') \rangle$, where $L(t)$ is a Langevin force with $\langle L(t) \rangle = 0$. Although the friction force and the correlation function are generally time-dependent we postulate in the following that the friction force has a constant intensity γ and introduce the Markovian approximation $b(t-t') = b_0 \delta(t-t')$. This assumption is only justified in the limit of large temperature, i.e. $b_0/2\gamma \gg 1$. We have checked that it does not change any physical conclusions concerning our work by implementing also finite-time correlation functions $b(t-t')$. We shall come back to the validity of time locality in the framework of the study presented in section 4. We also suppose that the

coupling to the environment is switched on only over the time interval during which the driving force is acting on the HO. This is the case in many situations of practical interest as, for instance, in the study of the excitation of Rydberg atoms during their passage through microwave cavities [2, 3]. Finally we restrict our study to the case of underdamped motion of the HO, i.e. $\omega_0 > \lambda = \gamma/2\mu$, which is the most interesting one in practice.

3.1. Classical energy distribution

In the classical case the equation of motion of the driven HO is now the following Langevin equation

$$\mu \ddot{q}_{cl}(t) + \gamma \dot{q}_{cl}(t) + \mu \omega_0^2 q_{cl}(t) = f(t) + L(t). \quad (3.1)$$

The initial condition is chosen to be the same as in (2.2), and for the same reason. Since the classical solution depends linearly on the force $L(t)$ and since this quantity is Gaussian distributed, the phase-space distribution $\rho(q, p, \Delta t; I_0, \phi_0)$ of the HO at time Δt reads [15]

$$\begin{aligned} &\rho(q, p, \Delta t; I_0, \phi_0) \\ &= \frac{1}{2\pi (\|C\|)^{1/2}} \exp \left\{ -\frac{1}{2} (q - \langle q_{cl}(I_0, \phi_0, \Delta t) \rangle, p \right. \\ &\quad \left. - \langle p_{cl}(I_0, \phi_0, \Delta t) \rangle) \begin{pmatrix} C_{11} & C_{12} \\ C_{21} & C_{22} \end{pmatrix}^{-1} \begin{pmatrix} q - \langle q_{cl}(I_0, \phi_0, \Delta t) \rangle \\ p - \langle p_{cl}(I_0, \phi_0, \Delta t) \rangle \end{pmatrix} \right\} \quad (3.2) \end{aligned}$$

with $I_0 = \hbar/2$ and $0 \leq \phi_0 < 2\pi$. Here $\langle q_{cl}(I_0, \phi_0, \Delta t) \rangle$ is the averaged solution of (3.1) ($\langle p_{cl}(I_0, \phi_0, \Delta t) \rangle = \mu \langle \dot{q}_{cl}(I_0, \phi_0, \Delta t) \rangle$) and $\|C\|$ is the determinant of the classical covariance matrix C whose matrix elements are the different variances associated with the HO, i.e.

$$\begin{aligned} C_{11} &= \langle q_{cl}^2(I_0, \phi_0, \Delta t) \rangle - \langle q_{cl}(I_0, \phi_0, \Delta t) \rangle^2 \\ C_{12} &= C_{21} = \langle q_{cl}(I_0, \phi_0, \Delta t) p_{cl}(I_0, \phi_0, \Delta t) \rangle - \langle q_{cl}(I_0, \phi_0, \Delta t) \rangle \langle p_{cl}(I_0, \phi_0, \Delta t) \rangle \\ C_{22} &= \langle p_{cl}^2(I_0, \phi_0, \Delta t) \rangle - \langle p_{cl}(I_0, \phi_0, \Delta t) \rangle^2. \quad (3.2a) \end{aligned}$$

The final probability distribution in energy is then

$$\begin{aligned} P^{CL,d}(E_f, \Delta t) &= \frac{1}{2\pi} \int_0^{2\pi} d\phi_0 \int_{-\infty}^{+\infty} dq \int_{-\infty}^{+\infty} dp \\ &\times \delta(E_f - (p^2/2\mu + \mu \omega_0^2 q^2/2)) \rho(q, p, \Delta t; I_0, \phi_0). \quad (3.3) \end{aligned}$$

This expression is easily computed numerically by using the usual transformation $q = \sqrt{2E_f/\mu\omega_0^2} \cos \phi_f$, $p = \sqrt{2\mu E_f} \sin \phi_f$ and replacing the double integration over q and p by a single one over ϕ_f .

Figure 1 shows also a typical energy distribution $\{P^{CL,d}(E_f, \Delta t)\}$. The coupling of the driven HO to the environment induces simultaneously two competing effects on

the distribution. While friction lowers the mean energy of the HO, diffusion broadens its energy distribution and therefore allows the HO to reach final energies beyond the dynamical barriers well inside the previously forbidden regions of phase space. This behaviour is reminiscent of the phenomenon first discussed by Kramers [16] in connection with classical transmission over a potential barrier due to the interaction with an environment. As expected, for asymptotic times (and $f(t)$ acting only over a finite interval of time), (3.3) reduces to the usual Boltzmann equilibrium distribution

$$P^{\text{CL,d}}(E_f, \infty) = (2\gamma\omega_0/b_0) \exp(-2\gamma E_f/b_0) \quad (3.4)$$

where the ratio $2\gamma/b_0$ may be interpreted as an inverse equilibrium temperature β (Einstein's relation).

3.2. Quantum energy distribution

If the quantum driven HO is coupled to the dissipative environment the occupation probability of a state n at time Δt , the HO being initially in the state m , is given by

$$P_{mn}^{\text{QM,d}}(\Delta t) = \int_{-\infty}^{+\infty} dq_0 \int_{-\infty}^{+\infty} dq'_0 \int_{-\infty}^{+\infty} dq_f \int_{-\infty}^{+\infty} dq'_f \varphi_n^*(q_f) \varphi_n^*(q'_f) \\ \times K(q_f, q'_f, \Delta t | q_0, q'_0, 0) \varphi_m(q_0) \varphi_m(q'_0) \quad (3.5)$$

where the φ_k 's are the eigenfunctions of the HO and K is the double propagator which describes the evolution from some initial point $q_0(q'_0)$ to a final point $q_f(q'_f)$. Its explicit expression is [14, 17, 18]

$$K(q_f, q'_f, \Delta t | q_0, q'_0, 0) = \int_{q_0}^{q_f} \mathcal{D}q(t) \int_{q'_0}^{q'_f} \mathcal{D}q'(t) \exp[i(S(q) - S(q'))/\hbar] \rho(q, q') \quad (3.6)$$

and involves a double integral over the paths $q(t)$ and $q'(t)$ with fixed boundaries (q_0, q_f) and (q'_0, q'_f) respectively. Here $S(q)$ is the action of the HO,

$$S(q) = \int_0^{\Delta t} dt \mathcal{L}(q, \dot{q}) \quad (3.7)$$

with $\mathcal{L}(q, \dot{q}) = \mu\dot{q}^2/2 - \mu\omega_0^2 q^2/2$, and $\rho(q, q')$ is the influence functional which takes into account the coupling to the environment and to the external driving force. Its expression reads

$$\rho(q, q') = \exp \left\{ \frac{i}{\hbar} \int_0^{\Delta t} dt' \left[-\frac{\gamma}{2} (q(t') - q'(t')) (\dot{q}(t') + \dot{q}'(t')) + (q(t') - q'(t')) f(t') \right] \right. \\ \left. - \frac{1}{2\hbar^2} \int_0^{\Delta t} dt' (q(t') - q'(t')) \int_0^{\Delta t} dt'' (q(t'') - q'(t'')) b(t' - t'') \right\} \quad (3.8)$$

where the friction coefficient γ and the correlation function $b(t - t') = b_0 \delta(t - t')$ are the same as in the classical case. This influence functional can be derived from transport models [18]. Here we postulate it, hence it is different from the influence functional obtained in [19] since it has not been derived through an explicit description of the environment. One can show that it leads to a differential equation for the density matrix which is the same as the one derived in [20].

The double propagator K can be worked out analytically [21] as the continuum limit of the discretized expression of (3.6). It can be written as

$$K = \mathbb{C} \exp(\Phi) \quad (3.9)$$

The explicit expressions for \mathbb{C} and Φ depend on the parameters of the model and on specific integrals of the driving force. The real constant \mathbb{C} takes care of the quantum fluctuations around the stationary classical paths which contribute to the complex phase Φ . Both quantities are found in appendix A where, for the sake of completeness, Φ is given for an arbitrary correlation function $b(t - t')$.

Using expression (3.9) in (3.5) it is possible to work out the non-perturbative compact analytic expression of the occupation probabilities $P_{0n}^{\text{QM},d}(\Delta t)$ we are interested in here. Since this expression is rather cumbersome and since its behaviour is not easy to understand by simple inspection, we present it in appendix B where we also give the essential steps of its derivation.

The expression (B.3) of the occupation probabilities $P_{0n}^{\text{QM},d}(\Delta t)$ that is obtained is well suited for numerical applications. Figure 2 displays a typical probability distribution $\{P_{0n}^{\text{QM},d}(\Delta t)\}$. One sees that the generalized 'tunnelling' effect responsible for the tail of the quantum energy distribution is clearly affected by the noisy environment.

As already done in figures 1 and 2, we choose the driving force to be constant for the remainder of the paper, i.e.

$$\begin{aligned} f(t) &= f_0 & \text{for } 0 \leq t \leq \Delta t \\ &= 0 & \text{otherwise} \end{aligned} \quad (3.10)$$

which, using (2.3a) and (2.7a), gives

$$W^2(\Delta t) = (W_{\text{max}}^2/2)(1 - \cos(\omega_0 \Delta t)) \quad (3.11)$$

with

$$W_{\text{max}}^2 = 2f_0^2 / \mu \hbar \omega_0^3. \quad (3.11a)$$

The quantity $W^2(\Delta t)$ is periodic for this choice, and therefore one can increase the time interval in steps of $2\pi/\omega_0$ without affecting either P^{CL} or P^{QM} . It is seen that the energy E_{max} of the upper barrier (cf (2.5)) reaches its maximum value $E_{\text{max}} = E_0(1 + \sqrt{2W_{\text{max}}^2})^2$ at times $\Delta t = (\pi/\omega_0)(2r + 1)$ (r integer).

3.3. Properties of the quantum occupation probabilities

We give here some properties characterizing the occupation probabilities $P_{0n}^{\text{QM},d}(\Delta t)$ and the conclusions which may be drawn from them.

3.3.1. *Mean energy.* It can be checked that the analytic expression of the mean quantum energy

$$\langle E(\Delta t) \rangle = E_0 \left(1 + 2 \sum_{n=0}^{\infty} n P_{0n}^{\text{QM,d}}(\Delta t) \right) \quad (3.12a)$$

of the HO coincides with the corresponding mean classical energy

$$\langle E(\Delta t) \rangle = \frac{1}{2\pi} \int_0^{2\pi} d\phi_0 \left(\frac{1}{2\mu} \langle p_{\text{cl}}^2(I_0, \phi_0, \Delta t) \rangle + \frac{\mu\omega_0^2}{2} \langle q_{\text{cl}}^2(I_0, \phi_0, \Delta t) \rangle \right) \quad (3.12b)$$

calculated from the solution of (3.1) together with the initial condition (2.2). Introducing the useful parameter $x = (b_0/\hbar\omega_0\gamma) - 1$, this expression may be written as

$$\langle E(\Delta t) \rangle = E_0 \left(1 + 2S^2(\Delta t) + x \left[(1 - e^{-2\lambda\Delta t}) - e^{-2\lambda\Delta t} \left(\frac{2\lambda^2}{\omega_0^2 - \lambda^2} \right) \sin^2 \left(\sqrt{\omega_0^2 - \lambda^2} \Delta t \right) \right] \right) \quad (3.13)$$

with

$$S^2(\Delta t) = \left(\frac{W_{\text{max}}^2}{4} \right) \left\{ \left[1 - e^{-\lambda\Delta t} \left(\cos \left(\sqrt{\omega_0^2 - \lambda^2} \Delta t \right) + \left(\frac{\lambda}{\sqrt{\omega_0^2 - \lambda^2}} \right) \sin \left(\sqrt{\omega_0^2 - \lambda^2} \Delta t \right) \right) \right]^2 + \left(\frac{\omega_0^2}{\omega_0^2 - \lambda^2} \right) e^{-2\lambda\Delta t} \sin^2 \left(\sqrt{\omega_0^2 - \lambda^2} \Delta t \right) \right\}. \quad (3.13a)$$

Such a result is expected [22] and supports the remark already made in the introduction, that the differences between the classical and quantum descriptions are manifested in the finer details of the occupation probability distribution. This check is nevertheless of importance because it shows that (3.8) is indeed the appropriate influence functional to describe the effects on a quantum system of a Markovian environment acting through friction and diffusion.

3.3.2. *Equilibrium.* When Δt goes to infinity the driven HO relaxes towards equilibrium and expression (B.3) then reads

$$P_{0n}^{\text{QM,d}}(\infty) = \left(\frac{2}{x+2} \right) \left(\frac{x}{x+2} \right)^n L_n^0 \left(\frac{-W_{\text{max}}^2}{x(x+2)} \right) \exp \left(-\frac{W_{\text{max}}^2}{2(x+2)} \right) \quad (3.14)$$

where L_n^0 is the Laguerre polynomial of order n . If, however, the driving force acts only over a finite time, (3.14) reduces to the usual Boltzmann occupation probability

$$P_{0n}^{\text{QM,d}}(\infty) = \left(\frac{2}{x+2} \right) \left(\frac{x}{x+2} \right)^n \sim \exp \left(-\beta \left(n + \frac{1}{2} \right) \hbar\omega_0 \right) \quad (3.15)$$

where the quantity β plays the role of an inverse equilibrium temperature which fulfils the quantum version of Einstein's relation, i.e.

$$\frac{b_0}{\gamma} = \hbar\omega_0 \coth\left(\frac{\beta\hbar\omega_0}{2}\right). \quad (3.16)$$

One sees that (3.15) and (3.16) are meaningful expressions only if $x \geq 0$, that is to say $b_0/\gamma \geq \hbar\omega_0$. For a given diffusion coefficient b_0 , this condition constraints the friction coefficient γ to lie in the interval $[0, b_0/\hbar\omega_0]$ (with $b_0/\hbar\omega_0 < 2\mu\omega_0$ because the motion is underdamped). (3.16) shows that the smaller γ the better the Markovian approximation (high temperature limit).

3.3.3. Short-time limit. In the limiting case $\gamma = b_0 = 0$ the general expression (B.3) reduces as expected to (2.7). On the other hand, if γ and b_0 are both fixed and Δt tends towards zero, one may expand (B.3) to first order in $\lambda = \gamma/2\mu$ and b_0 . This is the short-time limit of the occupation probabilities $P_{0n}^{\text{QM},d}$. It reads

$$\begin{aligned} P_{0n}^{\text{QM},d}(\Delta t) = & \frac{\exp(-W^2(\Delta t))}{n!} \left(W^{2n}(\Delta t) + (\lambda\Delta t)\{W^{2n}(\Delta t)[1 + ns(\Delta t)] \right. \\ & - W^{2(n-1)}(\Delta t)[n(n-1)s(\Delta t) + n] \\ & + \left. \left(\frac{b_0\Delta t}{2\mu\hbar\omega_0} \right) \left\{ W^{2(n+1)}(\Delta t)s(\Delta t) - W^{2n}(\Delta t)[1 + 2ns(\Delta t)] \right. \right. \\ & \left. \left. + W^{2(n-1)}(\Delta t)[n(n-1)s(\Delta t) + n] \right\} \right) \end{aligned} \quad (3.17)$$

with

$$s(\Delta t) = 1 + \frac{\sin(\omega_0\Delta t)}{\omega_0\Delta t}. \quad (3.17a)$$

For large quantum numbers n , (3.17) approximately reads

$$P_{0n}^{\text{QM},d}(\Delta t) \simeq P_{0n}^{\text{QM}}(\Delta t) \left[1 + x \left(\frac{n^2}{W_{\text{max}}^2} \right) (\lambda\Delta t) \right]. \quad (3.18)$$

One sees that the condition $x \geq 0$ implies the inequality $P_{0n}^{\text{QM},d}(\Delta t) \geq P_{0n}^{\text{QM}}(\Delta t)$ for n large. As seen in figure 2 this inequality is not restricted to the case considered in (3.18) but remains valid more generally, for Δt finite and n not very large.

4. Study of the behaviour of the dissipative driven HO above the dynamical barrier

With the help of some numerical examples where the parameters γ , b_0 and Δt are varied independently, we study now the effects of the noisy environment on the generalized 'tunnelling' process through the dynamical barrier of energy E_{max} . We first identify the two extreme regimes which characterize the dissipative driven HO. We then examine the behaviour of the tunnelling tail of the energy distribution $\{P_{0n}^{\text{QM},d}(\Delta t)\}$ by proceeding in two different (yet complementary) ways. On the one hand, the comparison between the occupation probabilities $P_{0n}^{\text{QM},d}(\Delta t)$ and $P_{0n}^{\text{QM}}(\Delta t)$ enables us to study how the occupation of the HO levels is affected by the environment. On the other hand, the comparison between the occupation probabilities $P_{0n}^{\text{QM},d}(\Delta t)$ and $P_{0n}^{\text{CL},d}(\Delta t)$ allows us to discuss the effect of dissipation on quantum phase coherence.

4.1. Extreme regimes of the dissipative HO

According to (3.16), for a given value of the diffusion coefficient b_0 the friction coefficient γ has to take values within the interval $[0, b_0/\hbar\omega_0]$. As shown in figure 3, the tunnelling tail of the distribution $\{P_{0n}^{\text{QM}}(\Delta t)\}$ lies between the two extreme distributions corresponding to the boundaries of the interval. Although rather unphysical, these two extreme regimes deserve to be mentioned because they set the bounds of the effect of the dissipative environment on the driven HO.

In the so-called diffusive regime, which corresponds to $\gamma \simeq 0$, the diffusion effect is the strongest. This is also the regime where the Markovian approximation is working (see discussion at the beginning of section 3). The expression of the occupation probabilities $P_{0n}^{\text{QM,d}}(\Delta t)$ is given by the leading order of the expansion of (B.3) as a function of γ . In this limit, the mean energy (3.13) reads

$$\langle E(\Delta t) \rangle = E_0 (1 + 2W^2(\Delta t)) + D\Delta t \quad (4.1)$$

where $D = b_0/2\mu$ is the momentum diffusion constant associated with the classical variance C_{22} . As expected, the mean energy is always larger than the one corresponding to the absence of coupling (cf (2.8a)), and a similar conclusion holds for the energy variance. Therefore, in the diffusive limit, the probabilities $P_{0n}^{\text{QM,d}}$ are larger than the probabilities P_{0n}^{QM} above the barrier.

The other extreme regime, which is called dissipative in the sequel, corresponds to the case for which the friction coefficient takes its maximally allowed value $\gamma = b_0/\hbar\omega_0$. If in this case γ becomes large (ω_0 small compared to b_0) the Markovian approximation may break down; since, however, we checked that this approximation does not invalidate the conclusions (see discussion at the beginning of section 3), we discuss this regime here for the sake of completeness. The occupation probabilities reduce to the remarkably simple Poissonian expression

$$P_{0n}^{\text{QM,d}}(\Delta t) = \frac{1}{n!} S^{2n}(\Delta t) \exp(-S^2(\Delta t)) \quad (4.2)$$

where $S^2(\Delta t)$ has been defined in (3.13a). The comparison between $W^2(\Delta t)$ (cf 3.11) and $S^2(\Delta t)$ shows that the condition $W^2(\Delta t) > S^2(\Delta t)$ is usually satisfied by choosing the time Δt adequately. This means that both the mean energy and the energy variance are usually smaller in the dissipative case than in the case without coupling. Hence, for $\gamma = b_0/\hbar\omega_0$, the probabilities $P_{0n}^{\text{QM,d}}$ are usually smaller than the probabilities P_{0n}^{QM} above the barrier. In the case where the friction coefficient γ is not equal to the limiting value $b_0/\hbar\omega_0$ but close to it, the tail of the associated distribution does not completely fall under the tail of the distribution $\{P_{0n}^{\text{QM}}(\Delta t)\}$. The two tails cross near a critical quantum number n^* (for instance $n^* = 9$ in figure 2). Numerical examples show that n^* increases with W_{max}^2 but decreases as x increases. An analytic expression of $n^*(\Delta t)$ may be given in the case of the short-time limit. Equating expressions (2.7) and (3.17), one gets

$$n^*(\Delta t) = \text{Int} \left\{ \left(\frac{W^2(\Delta t)}{2x} + \left(\frac{s(\Delta t) - 1}{2s(\Delta t)} \right) \right) + W^2(\Delta t) \right. \\ \left. + \sqrt{\left(\frac{W^2(\Delta t)}{2x} + \left(\frac{s(\Delta t) - 1}{2s(\Delta t)} \right) \right)^2 + W^2(\Delta t)} \right\} \quad (4.3)$$

where $\text{Int}\{y\}$ is the integer part of y and where $s(\Delta t)$ has been defined in (3.17a).

The considerations of this section allow us to conclude that, as the ordinary tunnelling phenomenon, the generalized 'tunnelling' process is reduced (enhanced) by the effect due to friction (diffusion). This rough picture will be improved in the next section.

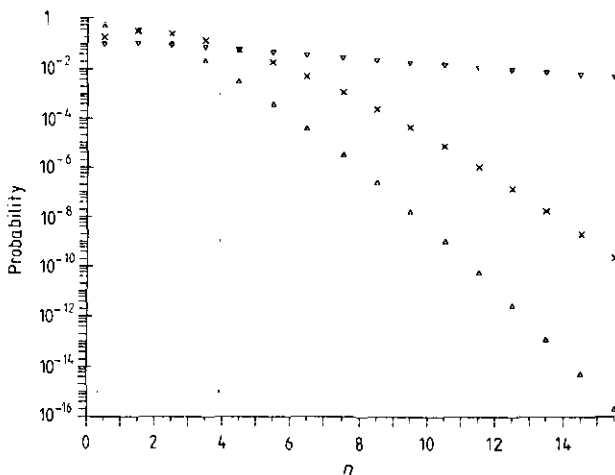


Figure 3. Quantum energy distributions corresponding to the two extreme regimes introduced by the consistency condition (see text), as a function of the HO quantum number n . The upper curve (∇) corresponds to the diffusive regime $\gamma = 0$ and the lower curve (Δ) to the dissipative regime $\gamma = b_0/\hbar\omega_0$. The distribution $\{P_{0n}^{\text{QM}}(\Delta t)\}$ (\times) is shown for comparison. The two vertical lines correspond to the two dynamical barriers. The parameters used here are $\mu = 0.5$, $\hbar = 1.0$, $\omega_0 = 1.5$, $b_0 = 2.2$, $f_0 = 1.5$ and $\Delta t = 3.0$.

4.2. Comparison between the quantum occupation probabilities with and without environment

The competing effects of friction and diffusion, on the one hand, and the conservation of total probability, on the other hand, give rise to opposite trends of the tunnelling tail of the distribution $\{P_{0n}^{\text{QM},d}(\Delta t)\}$ in the vicinity of the barrier, depending whether the system is near the dissipative limit or near the diffusive limit. This may be seen by studying, for a given diffusion coefficient b_0 and for a given time Δt , how the first normalized ratios $P_{0n}^{\text{QM},d}/P_{0n}^{\text{QM}}$ above the energy barrier are behaving as the friction coefficient γ decreases within the allowed interval $[0, b_0/\hbar\omega_0]$. Figures 4 and 5 show that, in the neighbourhood of the dissipative limit $\gamma \simeq b_0/\hbar\omega_0$ (here on the right of the graphs), a decrease of the coefficient γ produces a continuous increase of these ratios. Such a population behaviour is expected and easy to explain. As the value of the coefficient γ diminishes, the effect due to friction decreases in importance if compared with the effect due to diffusion and the ability of the system to reach energies above the barrier is increasing in consequence. Quite on the contrary, the same graphs show that in the neighbourhood of the diffusive limit $\gamma \simeq 0$ a decrease of the coefficient γ leads to a continuous decrease of the ratios $P_{0n}^{\text{QM},d}/P_{0n}^{\text{QM}}$. This depopulation behaviour originates from the conservation of the total probability. The

effect due to diffusion prevails now completely over the effect due to friction and the tail of the distribution flattens out more and more as one goes along towards the diffusive limit. But this possibility to reach higher and higher energies above the barrier occurs of course at the expense of the individual occupation probabilities $P_{0n}^{QM,d}$ in the energy region around the barrier, whose values have to diminish in order for the total occupation probability to remain constant.

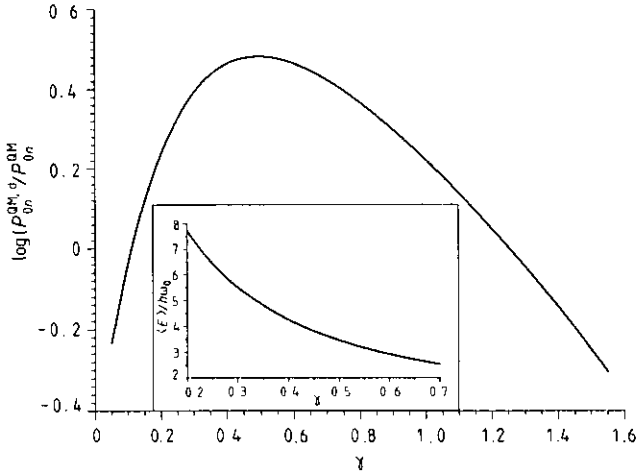


Figure 4. Logarithm of the ratio $P_{0n}^{QM,d}/P_{0n}^{QM}$ for $n = 3$ (corresponding to the first HO state above the dynamical barrier), as a function of the friction coefficient γ . The inset shows the variation of the ratio $\langle E \rangle / \hbar \omega_0$ with the coefficient γ . The parameters used here are $\mu = 0.5$, $\hbar = 1.0$, $\omega_0 = \pi/2$, $b_0 = 5.0$, $f_0 = 1.0$ and $\Delta t = 6.0$.

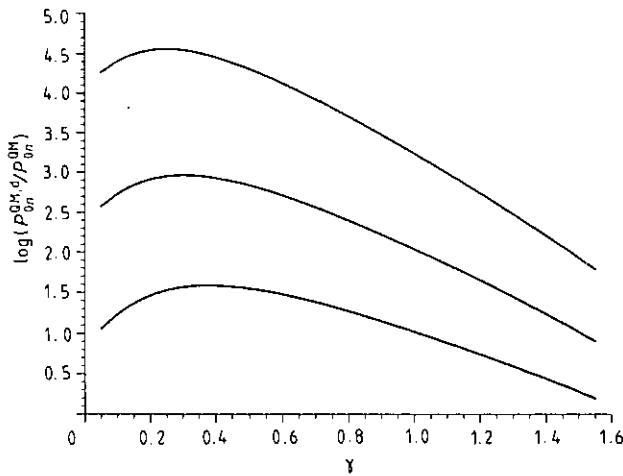


Figure 5. Logarithm of the ratios $P_{0n}^{QM,d}/P_{0n}^{QM}$ for $n = 4$ (lower curve), $n = 5$ (middle curve) and $n = 6$ (upper curve), as a function of the friction coefficient γ . The parameters are the same as those used in figure 4.

The diffusion coefficient and the time Δt being fixed, it is natural to ask for the value γ^* of the friction coefficient γ for which the transition from the population to the depopulation behaviour occurs above the barrier. In fact, a different value γ^* has to be associated with each individual HO state which is considered. The inset in figure 4 displays the variation of the mean energy $\langle E \rangle$ of the HO (cf (3.13)) as the value of the coefficient γ is modified. It shows that, starting near the dissipative regime, a progressive decrease of the coefficient γ produces as expected an increase of $\langle E \rangle$. From the study of many numerical examples, one finds that once $\langle E \rangle$ has increased enough as to be equal to the energy of a given state n , i.e. when

$$\frac{\langle E \rangle}{\hbar\omega_0} = n + \frac{1}{2} \quad (4.4)$$

the transition between the two behaviours occurs for this particular state. Indeed, it can be checked on the examples of figures 4 and 5 that the value γ^* of the coefficient γ for which the condition (4.4) is satisfied (see inset in figure 4) is exactly the same as the one for which the level n starts to be depopulated after having been continuously populated. The value of γ^* decreases with increasing n . In appropriate units, this value is $\gamma^* = 0.50$ for $n = 3$ (figure 4) and $\gamma^* = 0.38, 0.30, 0.25$ for $n = 4, 5, 6$ (figure 5).

There exists another way to observe, level by level, this transition from the population to the depopulation regime, which is much more suited for actual experiments. It consists in studying, for a given friction coefficient and a given diffusion coefficient (i.e. for a given temperature of the system), the variation with time Δt of the first normalized ratios $P_{0n}^{\text{QM},d} / P_{0n}^{\text{QM}}$ above the barrier. In order to do such a study in a transparent way one chooses the values of the successive times for which these ratios are computed as $\Delta t = (2\pi/\omega_0)(k + \xi)$, where k stands for an increasing integer while $0 < \xi < 1$. For this particular choice of the times Δt the probabilities P_{0n}^{QM} do not depend on k (because of the property of periodicity of the quantity $W^2(\Delta t)$, cf (3.11)), in contradistinction with the probabilities $P_{0n}^{\text{QM},d}$. One is therefore able, for a given HO state, to determine in an unambiguous manner the time Δt^* for which the expected transition happens. In practice, interpreting the relation (4.4) in a time-dependent picture, this time Δt^* has to correspond exactly to the time for which the value of the mean energy $\langle E(\Delta t) \rangle$ of the HO becomes equal to the value of the energy associated with the considered state. This is well confirmed by many numerical examples, among which the ones of figures 6 and 7. Indeed, reading on the graph $\langle E(\Delta t) \rangle$ in the inset of figure 6 the time value for which the mean energy reaches a given HO energy, one finds (in appropriate units) that $\Delta t^* = 4.1, 7.1, 10.6$ for $n = 2, 3, 4$, which is precisely the value for which the associated state ($n = 2$ in figure 6, $n = 3, 4$ in figure 7) starts to be depopulated. It takes obviously longer for $\langle E(\Delta t) \rangle$ to reach larger values and therefore the higher the state, the later the change from population to depopulation behaviour.

The succession in time of these two regimes may be interpreted as the succession in time of two different processes. As long as $\Delta t < \Delta t^*$ there is an effective competition between the effects due to friction and diffusion, and the level is populated through the generalized 'tunnelling' process. When $\Delta t > \Delta t^*$ the effect due to diffusion is completely prevailing over the effect due to friction. Therefore the process which depopulates the level has rather to be viewed as a diffusion-induced transmission through the barrier which can be considered as the quantum counterpart

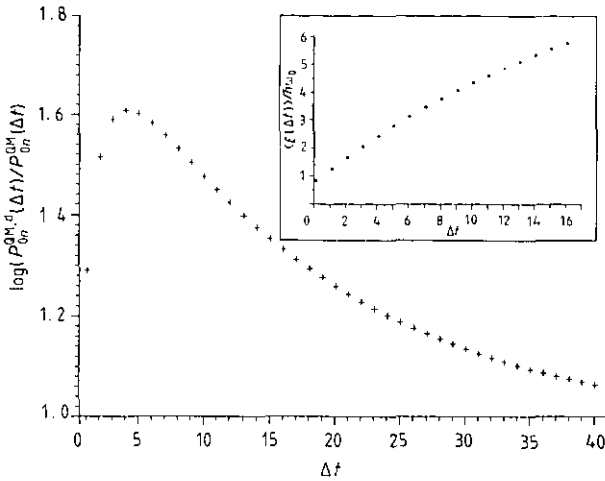


Figure 6. Logarithm of the ratio $P_{0n}^{QM,d}(\Delta t)/P_{0n}^{QM}(\Delta t)$ for $n = 2$ (corresponding to the first HO state above the dynamical barrier), for the successive times $\Delta t = (2\pi/\omega_0)(k + \xi)$ with $k = 0, 1, 2$ etc. The inset shows the variation of the ratio $\langle E(\Delta t) \rangle / \hbar\omega_0$ with these times Δt . The parameters used here are $\mu = 2.0$, $\hbar = 0.25$, $\omega_0 = 2\pi$, $\gamma = 0.1$, $b_0 = 3.0$, $f_0 = 13.5$ and $\xi = 0.1$.

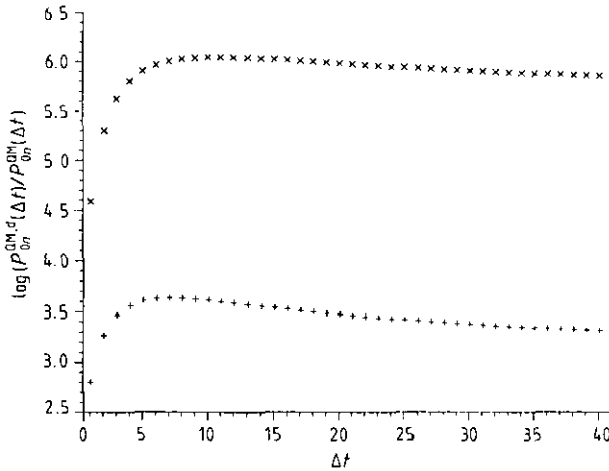


Figure 7. Logarithm of the ratios $P_{0n}^{QM,d}(\Delta t)/P_{0n}^{QM}(\Delta t)$ for $n = 3$ (lower curve) and $n = 4$ (upper curve), for the successive times $\Delta t = (2\pi/\omega_0)(k + \xi)$ with $k = 0, 1, 2$ etc. The parameters are the same as those used in figure 6.

of the classical Kramers diffusion. This picture will be corroborated by the results of the next section.

The population–depopulation transitions are observed above the barrier only when the mean energy has time enough to reach E_{\max} before it relaxes to equilibrium. Of course, as shown by (3.13), the larger the friction coefficient γ the longer the time needed by $\langle E(\Delta t) \rangle$ to cross the dynamical barrier. Therefore the smaller this coefficient the more pronounced the effect, i.e. the larger the number of levels for which the transition takes place. Hence it is in the vicinity of the diffusive regime,

when the Markovian assumption is best justified, that the effect is most favourably seen.

Several analytic results, which are relevant to the population–depopulation transition, may be derived close to the diffusive limit. For simplicity, they are given in the case for which the value of E_{\max} is the largest. The minimal time $(\Delta t)_{\min}$ which is needed for the mean energy to reach the barrier is obtained by equating the expression (4.1) to the expression of E_{\max} (cf (2.5)). One gets

$$(\Delta t)_{\min} = \left(\frac{2E_0}{D} \right) \sqrt{2W_{\max}^2}. \quad (4.5)$$

This time sets the lower bound of the transition times Δt^* . The expression of the mean energy which is valid close to the diffusive limit is obtained by taking the two lowest orders in the expansion of (3.13) in powers of λ . It reads

$$\langle E(\Delta t) \rangle = E_0 (1 + 2W_{\max}^2 + 2(x - W_{\max}^2)\lambda\Delta t). \quad (4.6)$$

Equating this last expression to the expression of E_{\max} one obtains the minimal time Δt needed by the mean energy (4.6) to reach the barrier, which (for $x > W_{\max}^2$) is given by

$$\Delta t = \frac{\sqrt{2W_{\max}^2}}{\lambda(x - W_{\max}^2)}. \quad (4.7)$$

On the other hand, the time Δt^* at which a state of given quantum number n above the barrier undergoes the transition from the population to the depopulation regime is obtained by equating the expression (4.6) to the expression $E_n = E_0(1 + 2n)$ of the energy of the state. It reads

$$\Delta t^* = \frac{n - W_{\max}^2}{\lambda(x - W_{\max}^2)}. \quad (4.8)$$

For $n, x \gg W_{\max}^2$, the time Δt^* is approximately given by

$$\Delta t^* \simeq \frac{E_n}{D - 2\lambda E_0}. \quad (4.8a)$$

Finally, it is interesting to get an idea of the number of levels which are undergoing the transition before relaxation of the mean energy occurs. The expression (3.13) shows that $(\Delta t)_r = 1/2\lambda$ is a typical relaxation time of $\langle E(\Delta t) \rangle$. Equating $(\Delta t)_r$ to the expression (4.8) of Δt^* , one gets approximately the quantum number N of the highest state for which the transition is still clearly seen

$$N = \text{Int} \left\{ \frac{x}{2} + \frac{W_{\max}^2}{2} \right\} \quad (4.9)$$

which, for $x \gg W_{\max}^2$, may be written as

$$N \simeq \text{Int} \left\{ \frac{D}{2E_0} (\Delta t)_r \right\}. \quad (4.9a)$$

In numerical studies the minimal size of the density matrix describing the time evolution of a dissipative quantum system has clearly to be chosen of the order of N .

4.3. Comparison between the classical and quantum occupation probabilities

In order to complement the previous discussion, it is interesting to compare the tails of the distributions $\{P^{\text{CL},d}(E_f, \Delta t)\}$ and $\{P_{0n}^{\text{QM},d}(\Delta t)\}$ for various values of the parameters γ , b_0 and Δt . Indeed, such comparisons allow us to study the importance of the generalized 'tunnelling' process compared with the classical diffusive transmission through the dynamical barrier. They provide us therefore with a clear picture about how the noisy environment affects quantum phase coherence.

Figure 8 shows that, if compared to the classical diffusive transmission through the dynamical barrier, the generalized 'tunnelling' process decreases the ability of the system to reach energy values above E_{max} . This is the very fingerprint of phase coherence, whose effect is to reduce the values of the quantum occupation probabilities in comparison with the values of the classical occupation probabilities. This reduction becomes more important in proportion as energy increases. For the example of figure 8, the ratio $P^{\text{QM},d}/P^{\text{CL},d}$ is of the order of 0.8 for $n = 4$ and 0.7 for $n = 5$ whereas it is of the order of 0.04 for $n = 16$ and 0.03 for $n = 17$. Hence phase coherence is responsible for the localization in energy of the tail of the quantum distribution.

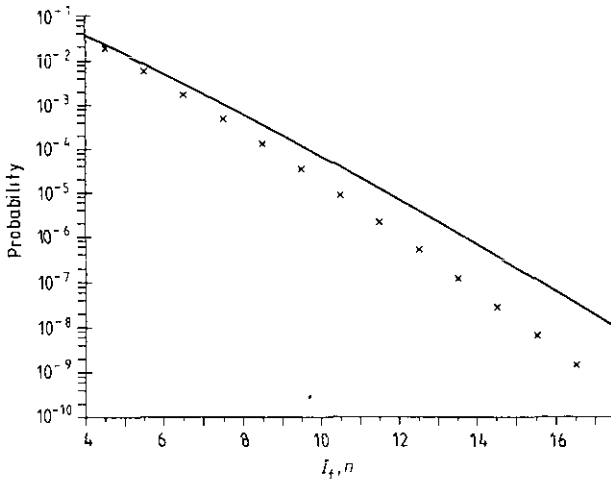


Figure 8. Comparison between the energy distributions $\{P^{\text{CL},d}(E_f, \Delta t)\}$ (full line) and $\{P_{0n}^{\text{QM},d}(\Delta t)\}$ (x) above the dynamical barrier. The classical (quantum) distribution is the same as in figure 1 (2) respectively.

The differences $\Delta(n) = P^{\text{CL},d}(E_f = E_n, \Delta t) - P_{0n}^{\text{QM},d}(\Delta t)$ provide a quantitative measure of the importance of the generalized 'tunnelling' process compared with the classical diffusive transmission. These quantities enable us to study in which manner quantum phase coherence is affected by variations of the friction and diffusion coefficients and of the time Δt . Figure 9 shows that, for a given diffusion coefficient and a given time Δt , the differences $\Delta(n)$ are decreasing as the friction coefficient γ increases, the decrease becoming more significant as the state n lies higher in energy. For the example of figure 9, this decrease between the cases $\gamma = 0.4$ and $\gamma = 1.0$ (in appropriate units) is of one order of magnitude for $n = 10$ whereas it is of three orders of magnitude for $n = 20$. This means

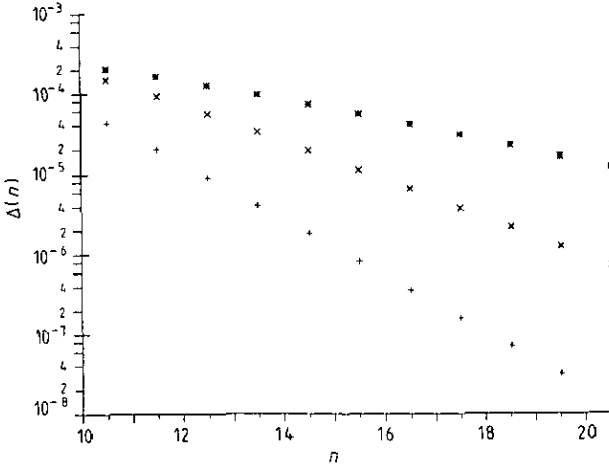


Figure 9. Differences $\Delta(n) = P_{0n}^{CL,d}(E_f = (n + 1/2)\hbar\omega_0) - P_{0n}^{QM,d}$ for HO states n above the dynamical barrier (the values of the differences are marked at $n + 1/2$), as a function of the friction coefficient γ . The lower curve corresponds to $\gamma = 1.0$, the middle one to $\gamma = 0.7$ and the upper one to $\gamma = 0.4$. The parameters used here are $\mu = 0.5$, $\hbar = 1.0$, $\omega_0 = 1.5$, $b_0 = 3.5$, $f_0 = 0.1$ and $\Delta t = 3.0$.

that the effect of quantum phase coherence is progressively weakened as the friction coefficient grows, and the more so the higher one goes in energy. In other words, the phenomenon of localization in energy of the quantum distribution becomes less apparent in proportion as the effect due to friction increases. So it is for $\gamma \simeq 0$, i.e. close to the diffusive limit, that this phenomenon is most clearly seen. In a complementary manner one can also examine the behaviour of the differences $\Delta(n)$ with respect to variations of the diffusion coefficient b_0 , for a given friction coefficient and a given time Δt . This is done in figure 10 which shows that the quantities $\Delta(n)$ are increasing with the coefficient b_0 . This increase becomes more pronounced if the considered energy is larger. Hence the phenomenon of localization in energy of the quantum distribution becomes more conspicuous as the effect due to diffusion gets more important.

The effect of quantum phase coherence on the occupation probabilities is changing with time. This is clearly seen in figure 11 which displays, for three different HO states n beyond the barrier, the variation of the difference $\Delta(n, \Delta t)$ as the time Δt increases in steps of $2\pi/\omega_0$ (the values of the different parameters are the same as in figures 6 and 7). As it was the case for the ratios $P_{0n}^{QM,d}(\Delta t)/P_{0n}^{QM}(\Delta t)$ (and for the same reasons, as seen below) the behaviour in time of the difference $\Delta(n, \Delta t)$ is characterized by two successive stages. In the first stage the effect of quantum phase coherence on the occupation probability of a given state is increasing in proportion as time grows. Indeed, the effect due to diffusion is gaining progressively in importance over the effect due to friction as time goes and so, according to what has been said above, the difference $\Delta(n, \Delta t)$ has to increase in consequence. On the contrary one sees that the effect of quantum phase coherence is decreasing with increasing time in the second stage. To find the origin of this behaviour it is crucial to observe in figure 11 the time at which the effect of phase coherence on the occupation probability of a state n starts to decrease after having increased. Looking at the

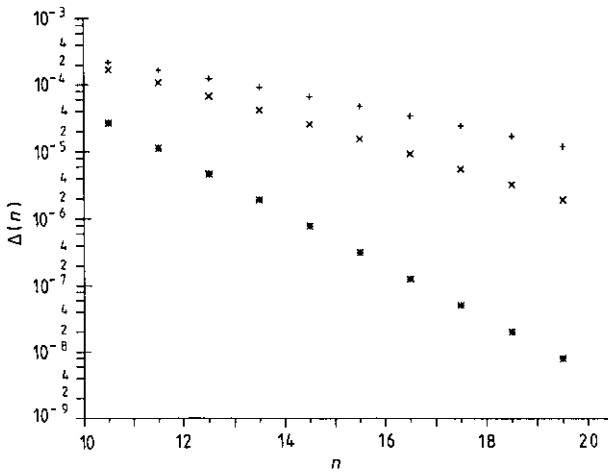


Figure 10. Differences $\Delta(n) = P^{\text{CL},d}(E_t = (n + 1/2)\hbar\omega_0) - P_{0n}^{\text{QM},d}$ for HO states n above the dynamical barrier, as a function of the diffusion coefficient b_0 . The lower curve corresponds to $b_0 = 3.0$, the middle one to $b_0 = 5.0$ and the upper one to $b_0 = 7.0$. The parameters used here are $\mu = 0.5$, $\hbar = 1.0$, $\omega_0 = 1.5$, $\gamma = 1.0$, $f_0 = 0.5$ and $\Delta t = 3.0$.

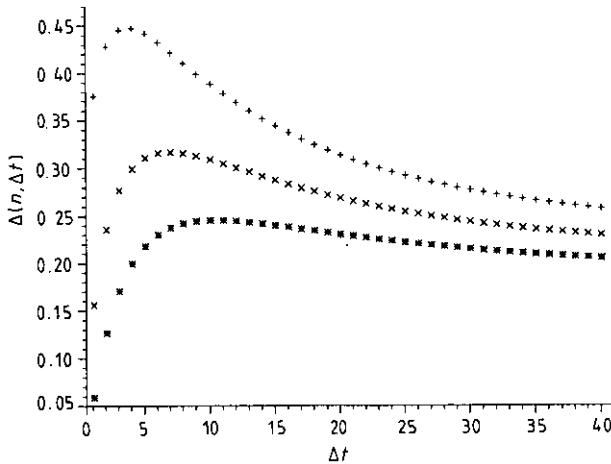


Figure 11. Differences $\Delta(n, \Delta t) = P^{\text{CL},d}(E_t = (n + 1/2)\hbar\omega_0, \Delta t) - P_{0n}^{\text{QM},d}(\Delta t)$ for HO states n beyond the dynamical barrier, for successive times $\Delta t = (2\pi/\omega_0)(k + \xi)$ with $k = 0, 1, 2$ etc. The upper curve is for $n = 2$, the middle one for $n = 3$ and the lower one for $n = 4$. The parameters are the same as those used in figures 6, 7.

inset of figure 6, one sees that this time corresponds once again precisely to the time for which the condition $\langle E(\Delta t) \rangle / \hbar\omega_0 = n + 1/2$ is satisfied, i.e. the time Δt^* at which the population–depopulation transition occurs for the state n . As a matter of fact one can check that, for the considered state, the time associated with the maximum of the curve is the same in figure 11 as in figures 6 and 7, i.e. $\Delta t^* = 4.1, 7.1, 10.6$ for $n = 2, 3, 4$. This coincidence allows us to conclude that the decrease of quantum phase coherence in the second stage has the same origin as the

depopulation behaviour, which is the conservation of the total occupation probability.

All these facts lead us to the conclusion that, for a given state, the population stage is also the stage for which the effect of quantum phase coherence on the occupation probability increases whereas the depopulation stage is, on the contrary, the stage for which the effect of quantum phase coherence is weakened. Hence the transition from a population to a depopulation behaviour also corresponds to a transition from an increase to a decrease of the effect of quantum phase coherence, occurring at the same time Δt^* .

This conclusion supports what has already been said in the previous section, that the existence of two stages in the occupation of a given energy level is the fingerprint of the succession in time of two different processes. Indeed, when $\Delta t < \Delta t^*$, the values of the classical and quantum occupation probabilities are moving away from each other as time increases. This is a clear indication that the level is populated by a different process in each case. It is the diffusive transmission in the classical case and, because the effect of phase coherence is enhanced in this stage, a genuine generalized 'tunnelling' process in the quantum case. In contrast the values of the classical and quantum occupation probabilities are moving closer to each other as time grows when $\Delta t > \Delta t^*$. This means that the level is depopulated by a process which, from a generalized 'tunnelling' phenomenon, tends progressively to become a quantum diffusion induced transmission through the barrier as the effect of phase coherence is weakened.

5. Conclusion

The purpose of this paper has been to study how the process of 'tunnelling' through an energy barrier of dynamical origin, which generalizes ordinary tunnelling through a potential barrier, is affected by the presence of a noisy environment. This has been done in the framework of a soluble model which consists of a driven HO (angular frequency ω_0) coupled to a Markovian environment (friction coefficient γ , diffusion coefficient b_0). The finite-time energy distribution of the quantum dissipative driven HO, which is the central quantity of interest in the study, has been expressed in closed analytic form without resorting to any approximation.

The comparison of the tail of the quantum energy distribution in the diffusive regime ($\gamma \simeq 0$) with the one in the dissipative regime ($\gamma = b_0/\hbar\omega_0$) shows that the generalized 'tunnelling' process through the dynamical barrier is enhanced (reduced) by the diffusion (friction) effect. This rough picture has been refined by studying how the individual HO levels above the dynamical barrier are occupied. The conservation of the total occupation probability implies that the occupation of a given level is characterized by two different stages occurring successively in time. The level is continuously populated (depopulated) in the first (second) stage. Going further, it has been shown that the transition from the population to the depopulation stage happens precisely at the time Δt^* at which the mean energy of the dissipative driven HO becomes equal to the energy of the considered level. An analytic expression of Δt^* , valid close to the diffusive limit where the Markovian description of the environment is best justified, has been given.

These results have been complemented by a quantitative comparison between the generalized 'tunnelling' process and the classical diffusive transmission through the barrier. Phase coherence localizes the tail of the quantum energy distribution

compared with the tail of the classical energy distribution. This localization effect becomes more (less) conspicuous as the diffusion (friction) coefficient is increased. The study of the effect of phase coherence on the occupation of a given HO level shows that the population (depopulation) stage is also the stage in which phase coherence is enhanced (weakened). As a consequence, a given level is populated by a genuine generalized 'tunnelling' process whereas it is depopulated by a process which can be considered as a quantum diffusion induced transmission through the barrier.

Acknowledgments

One of us (US) thanks the CRN for its kind hospitality. Discussions with Professor E Pollak are gratefully acknowledged.

Appendix A

In the case of underdamped motion of the HO ($\omega_0 > \lambda = \gamma/2\mu$), which is the one considered here, the pre-exponential factor \mathbb{C} and the phase Φ introduced in (3.9) read [21]

$$\mathbb{C} = \frac{\mu\sqrt{\omega_0^2 - \lambda^2} \exp(\lambda\Delta t)}{2\pi\hbar \sin(\sqrt{\omega_0^2 - \lambda^2}\Delta t)} \quad (\text{A.1})$$

and

$$\Phi = i\mu[\eta(\Delta t)\dot{Q}(\Delta t) - \eta(0)\dot{Q}(0)]/\hbar + \frac{1}{2\hbar^2} \int_0^{\Delta t} dt' \eta(t') \int_0^{\Delta t} dt'' \eta(t'') b(t' - t'') \quad (\text{A.2})$$

with $\eta(t) = q(t) - q'(t)$ and $Q(t) = (q(t) + q'(t))/2$.

Here $q(t)$ and $q'(t)$ are the solutions of the coupled saddle-point equations obtained from (3.6):

$$\begin{aligned} \frac{d}{dt} \left(\frac{\partial \mathcal{L}}{\partial \dot{q}(t)} \right) - \frac{\partial \mathcal{L}}{\partial q(t)} + \gamma \dot{q}'(t) - f(t) - \frac{i}{\hbar} \int_0^{\Delta t} dt' (q(t') - q'(t')) b(t - t') &= 0 \\ \frac{d}{dt} \left(\frac{\partial \mathcal{L}}{\partial \dot{q}'(t)} \right) - \frac{\partial \mathcal{L}}{\partial q'(t)} + \gamma \dot{q}(t) - f(t) - \frac{i}{\hbar} \int_0^{\Delta t} dt' (q(t') - q'(t')) b(t - t') &= 0 \end{aligned} \quad (\text{A.3})$$

where \mathcal{L} is the Lagrangian of the HO and the boundary conditions are fixed such that $q(0) = q_0$, $q'(0) = q'_0$, $q(\Delta t) = q_f$ and $q'(\Delta t) = q'_f$.

Solving these equations explicitly, it is possible to put the phase Φ into the following form

$$\begin{aligned} \Phi = A_1 \eta_f^2 + iA_2 \eta_f Q_f + iA_3 \eta_f + A_4 \eta_f \eta_0 + iA_5 \eta_f Q_0 \\ + iA_6 Q_f \eta_0 + iA_7 \eta_0 + iA_8 \eta_0 Q_0 + A_9 \eta_0^2 \end{aligned} \quad (\text{A.4})$$

where $\eta_0 = q_0 - q'_0$, $\eta_t = q_t - q'_t$, $Q_0 = (q_0 + q'_0)/2$ and $Q_t = (q_t + q'_t)/2$. The real time-varying coefficients A_i ($i = 1, 9$) depend either on γ alone (A_2, A_5, A_6, A_8) or on both γ and b_0 (A_1, A_4, A_9) or on both γ and $f(t)$ (A_3, A_7). Introducing the quantities

$$\alpha(t) = (\exp(\lambda_2 t + \lambda_1 \Delta t) - \exp(\lambda_1 t + \lambda_2 \Delta t)) / (\exp(\lambda_1 \Delta t) - \exp(\lambda_2 \Delta t)) \quad (\text{A.5})$$

and

$$\beta(t) = (\exp(\lambda_1 t) - \exp(\lambda_2 t)) / (\exp(\lambda_1 \Delta t) - \exp(\lambda_2 \Delta t)) \quad (\text{A.6})$$

with $\lambda_{1(2)} = \lambda + (-)i(\omega_0^2 - \lambda^2)^{1/2}$, these coefficients are given by the following general expressions

$$\begin{aligned} A_1 &= -\frac{1}{2\hbar^2} \int_0^{\Delta t} dt \beta(t) \int_0^{\Delta t} dt' \beta(t') b(t-t') \\ A_2 &= \frac{\mu}{\hbar} (\lambda_1 \exp(\lambda_2 \Delta t) - \lambda_2 \exp(\lambda_1 \Delta t)) / (\exp(\lambda_1 \Delta t) - \exp(\lambda_2 \Delta t)) \\ A_3 &= \frac{1}{\hbar} \int_0^{\Delta t} dt f(t) \beta(t) \\ A_4 &= -\frac{1}{\hbar^2} \int_0^{\Delta t} dt \beta(t) \int_0^{\Delta t} dt' \alpha(t') b(t-t') \\ A_5 &= \frac{\mu}{\hbar} (\lambda_2 - \lambda_1) / (\exp(\lambda_1 \Delta t) - \exp(\lambda_2 \Delta t)) \\ A_6 &= A_5 \exp(2\lambda \Delta t) \\ A_7 &= \frac{1}{\hbar} \int_0^{\Delta t} dt f(t) \alpha(t) \\ A_8 &= A_2 + \gamma / \hbar \\ A_9 &= -\frac{1}{2\hbar^2} \int_0^{\Delta t} dt \alpha(t) \int_0^{\Delta t} dt' \alpha(t') b(t-t'). \end{aligned} \quad (\text{A.7})$$

For the case of interest here, i.e. $b(t-t') = b_0 \delta(t-t')$, all these expressions can easily be worked out analytically.

Appendix B

We give here the general analytic expression of the quantum occupation probabilities $P_{0n}^{\text{QM},d}(\Delta t)$. To obtain it one starts with (3.5) and (3.9) (where \mathbb{C} and Φ are defined by (A.1) and (A.4) in appendix A) and with the HO wavefunctions

$$\varphi_n(q) = (2\nu/\pi)^{1/4} (2^n n!)^{-1/2} H_n((2\nu)^{1/2} q) \exp(-\nu q^2)$$

where H_n is the Hermite polynomial of order n and $\nu = \mu\omega_0/2\hbar$.

Changing variables to

$$x_0 = (2\nu)^{1/2}(q_0 + q'_0)/2$$

$$y_0 = (2\nu)^{1/2}(q_0 - q'_0)/2$$

$$x_t = (2\nu)^{1/2}(q_t + q'_t)/2$$

$$y_t = (2\nu)^{1/2}(q_t - q'_t)/2$$

it is possible to integrate over x_0 and x_t by using the identity [23]

$$\int_{-\infty}^{+\infty} dx \exp(-x^2 + ix\beta) H_n(x+y) H_n(x-y) \\ = 2^n \pi^{1/2} n! \exp(-\beta^2/4) L_n^0(2y^2 + \beta^2/2)$$

where L_n^0 is the Laguerre polynomial of order n .

One is therefore led to the intermediate expression

$$P_{mn}^{\text{QM},d}(\Delta t) = (2C/\nu) \text{Re} \left\{ \int_{-\infty}^{+\infty} dy_0 \int_{-\infty}^{+\infty} dy_t \right. \\ \times \exp(-ay_0^2 - by_t^2 + cy_0y_t + idy_0 + ie y_t) \\ \times L_m^0((2 + A_8^2/2\nu^2)y_0^2 + A_5^2y_t^2/2\nu^2 + A_5A_8y_0y_t/\nu^2) \\ \left. \times L_n^0((2 + A_2^2/2\nu^2)y_t^2 + A_6^2y_0^2/2\nu^2 + A_2A_6y_0y_t/\nu^2) \right\} \quad (\text{B.1})$$

where the quantities A_i are defined in appendix A and

$$a = (1 - b_0/\hbar\omega_0\gamma)(1 + A_8^2/4\nu^2) + (1 + b_0/\hbar\omega_0\gamma)(A_6^2/4\nu^2)$$

$$b = (1 + b_0/\hbar\omega_0\gamma)(1 + A_2^2/4\nu^2) + (1 - b_0/\hbar\omega_0\gamma)(A_5^2/4\nu^2)$$

$$c = -(1 - b_0/\hbar\omega_0\gamma)(A_5A_8/2\nu^2) - (1 + b_0/\hbar\omega_0\gamma)(A_2A_6/2\nu^2) \quad (\text{B.2})$$

$$d = 2A_7/(2\nu)^{1/2}$$

$$e = 2A_3/(2\nu)^{1/2}$$

(it may be shown that the quantities a and b are always positive as expected).

Considering the special case $m = 0$ we are interested in here (the general case can also be worked out directly), the previous expression is integrated in a straightforward way by using the polynomial expansion of L_n^0 together with an appropriate change of variables. The final result reads

$$P_{0n}^{\text{QM},d}(\Delta t) = \frac{1}{\sqrt{G_1}} \exp(-G_6/G_1) \sum_{i=0}^n C_i^n \frac{1}{i!} \left(\frac{\nu}{4}\right)^i \\ \times \sum_{j=0}^i C_j^i \left(\frac{1}{\nu^2}\right)^j \sum_{l=0}^{i-j} C_{2l}^{2i-2j} \frac{(2l)!}{l!} \left(\frac{1}{G_2}\right)^l \sum_{k=0}^{2j} C_k^{2j} \left(\frac{G_4}{G_1}\right)^{2j-k} \\ \times \sum_{p=0}^{2i-2j-2l} C_p^{2i-2j-2l} \frac{(k+p)!}{(k+p/2)!} \left(\frac{G_3}{G_2}\right)^p \left(\frac{G_2}{G_1}\right)^{(k+p/2)} \left(\frac{G_5}{G_1}\right)^{2i-2j-2l-p} \quad (\text{B.3})$$

where $C_i^n = n!/i!(n-i)!$ etc. and where the indices k and p have always to be of the same parity.

The time-varying quantities G_i ($i = 1, 6$) are most conveniently expressed in terms of the parameter $x = (b_0/\hbar\omega_0\gamma) - 1$. They are given by the following expressions ($\lambda = \gamma/2\mu$)

$$\begin{aligned}
 G_1 &= 1 + x\{1 - (1/2A_6^2)(8\nu^2 + A_2^2 + A_8^2)\} \\
 &\quad + x^2\{(A_5^2 + A_6^2 - (8\nu^2 + A_2^2 + A_8^2))/4A_6^2\} \\
 G_2 &= -\nu[1 + x\{(A_6^2 - 4\nu^2 - A_8^2)/2A_6^2\}] \\
 G_3 &= -x\{(\nu/A_6^2)(A_8 - A_2)\} \\
 G_4 &= (1/2A_6^2)[-2A_2A_6F_1 - 8\nu^2A_6F_2 + x\{(A_5A_8 - A_2A_6)F_1 \\
 &\quad + 4\nu^2(A_5 - A_6)F_2\}] \\
 G_5 &= (1/A_6^2)[2A_6F_1 - 2A_6A_8F_2 + x\{(A_6 - A_5)F_1 - (A_6A_8 - A_2A_5)F_2\}] \\
 G_6 &= (\nu/2A_6^2)[2((4\nu^2 + A_2^2)F_1^2/4\nu^2) + 2(4\nu^2 + A_8^2)F_2^2 - (8\lambda\mu F_1F_2/\hbar) \\
 &\quad + x\{((4\nu^2 + A_2^2 - A_5^2)F_1^2/4\nu^2) + (4\nu^2 + A_8^2 - A_5^2)F_2^2 \\
 &\quad - (4\lambda\mu F_1F_2/\hbar)\}]
 \end{aligned} \tag{B.4}$$

with

$$F_1 = \left(\frac{1}{\hbar}\right) \int_0^{\Delta t} dt f(t) e^{\lambda t} \left(\cos\left(\sqrt{\omega_0^2 - \lambda^2}t\right) + \left(\frac{\lambda}{\sqrt{\omega_0^2 - \lambda^2}}\right) \sin\left(\sqrt{\omega_0^2 - \lambda^2}t\right) \right)$$

and

$$F_2 = \left(\frac{1}{\mu\sqrt{\omega_0^2 - \lambda^2}}\right) \int_0^{\Delta t} dt f(t) e^{\lambda t} \sin\left(\sqrt{\omega_0^2 - \lambda^2}t\right).$$

One can check that $\sum_{n=0}^{\infty} P_{0n}^{\text{QM,d}}(\Delta t) = 1$, as it must be.

References

- [1] Leggett A J 1984 *Percolation, Localization and Superconductivity* (NATO ASI Series, Series B: Physics 109) ed A M Goldman and S A Wolf (New York: Plenum)
- [2] Bayfield J E and Sokol D W 1988 *Physics of Atoms and Molecules* ed K T Taylor, M K Naytch and C W Clark (New York: Plenum)
- [3] Blümel R, Graham R, Sirko L, Smilansky U, Wälther H and Yamada K 1989 *Phys. Lett.* **62** 341
- [4] Weidenmüller H A 1980 *Progress in Particle and Nuclear Physics* vol 3, ed D Wilkinson (Oxford: Pergamon)
- [5] Hänggi P, Talkner P and Borkovec M 1990 *Rev. Mod. Phys.* **62** 251
- [6] Caldeira A O and Leggett A J 1981 *Phys. Rev. Lett.* **46** 211; 1983 *Ann. Phys., NY* **149** 374
Wolynes P G 1981 *Phys. Rev. Lett.* **47** 968
Bray A J and Moore M A 1982 *Phys. Rev. Lett.* **49** 1545

- [7] Steadman S G (ed) 1985 *Fusion Below the Coulomb Barrier (Lecture Notes in Physics 219)* (Berlin: Springer)
- [8] Landau L D and Lifshitz E M 1992 *Quantum Mechanics* vol 3 (New York: Pergamon)
- [9] Shimshoni E and Gefen Y 1991 *Ann. Phys., Lpz.* **210** 16; and references therein
- [10] Miller WH 1974 *Adv. Chem. Phys. Vol XXV* ed I Prigogine and S A Rice (New York: Wiley)
- [11] Schaeffer R 1978 *Les Houches Summer School in Theoretical Physics Session XXX* ed R Balian, M Rho and G Ripka (Amsterdam: North-Holland)
- [12] Levit S, Smilansky U and Pelte D 1974 *Phys. Lett.* **53B** 139
- [13] Pechukas P and Child M S 1976 *Mol. Phys.* **31** 973
- [14] Feynman R P and Hibbs A R 1965 *Quantum Mechanics and Path Integrals* (New York: McGraw)
- [15] Fox R F 1978 *Phys. Rep.* **48** 179
- [16] Kramers H A 1940 *Physica* **7** 284
- [17] Feynman R P and Vernon A R 1963 *Ann. Phys., NY* **24** 118
- [18] Brink D M, Neto J and Weidenmüller H A 1979 *Phys. Lett.* **80B** 170
- [19] Grabert H, Schramm P and Ingold G L 1988 *Phys. Rep.* **168** 115
- [20] Caldeira A O and Leggett A J 1983 *Physica A* **121** 587
- [21] Sami T and Richert J 1986 *Nuovo Cimento A* **93** 159
- [22] Rips I and Pollak E 1990 *Phys. Rev. A* **41** 5366
- [23] Gradshteyn I S and Ryzhik I M 1965 *Tables of Integrals, Series, and Products* (New York: Academic) p 838